Phosphorus Analogues of [Ni(bpy)2]: Synthesis and Application in CarbontextendashHalogen Bond Activation

Leitl, J.; Coburger, P.; Scott, D.J.; Ziegler, C.G.P.; Hierlmeier, G.; Wolf, R.; van Leest, N.P.; Bruin, B. de; Hörner, G.; Müller, C.

DOI
10.1021/acs.inorgchem.0c01115

Publication date
2020

Document Version
Final published version

Published in
Inorganic Chemistry

Inorganic Chemistry

pubs.acs.org/IC Article

Phosphorus Analogues of [Ni(bpy)$_2$]: Synthesis and Application in Carbon−Halogen Bond Activation

J. Leitl, P. Coburger, D. J. Scott, C. G. P. Ziegler, G. Hierlmeier, R. Wolf,* N. P. van Leest, B. de Bruin,* G. Hörner, and C. Müller*

Cite This: *Inorg. Chem.* 2020, 59, 9951−9961 Read Online

ACCESS | Metrics & More | Article Recommendations | Supporting Information

ABSTRACT: The neutral, homoleptic pyridylphosphininenickel(0) complex [Ni(2-Py-4,6-Ph$_2$-PC$_5$H$_2$)$_2$] (**1**) has been obtained by reaction of the formal Ni(0) source [(IPr)Ni(H$_2$C═CHSiMe$_3$)$_2$] with 2 equiv of 2-(2′-pyridyl)-4,6-diphenylphosphinine (**L**). Compound **1** can be oxidized both electrochemically and through the use of ferrocenium salts, to afford the corresponding Ni(I) complexes [**1**]BF$_4$, [**1**(THF)]PF$_6$, and [**1**$_2$](BAr$^F_4$)$_2$. The structures of these salts reveal an interesting dependence on the nature of the anion. While [**1**]BF$_4$ and [**1**(THF)]PF$_6$ show trigonal-bipyramidal coordination of Ni in the solid state, [**1**$_2$](BAr$^F_4$)$_2$ exists as a dinuclear Ni(I) complex and possesses a bridging phosphinine moiety in a rare μ_2 mode. Reactions of **1** with halobenzenes highlight the noninnocent behavior of the aromatic phosphinine ligand, leading to the formation of oxidized Ni complexes but not to classical oxidative addition products. The reaction of **1** with bromobenzene affords the λ^5 phosphinine **2** and the bipyramidal Ni(I) complex [**1**]Br, whereas a more unconventional oxidation product **3** is formed from the reaction of **1** and iodobenzene.

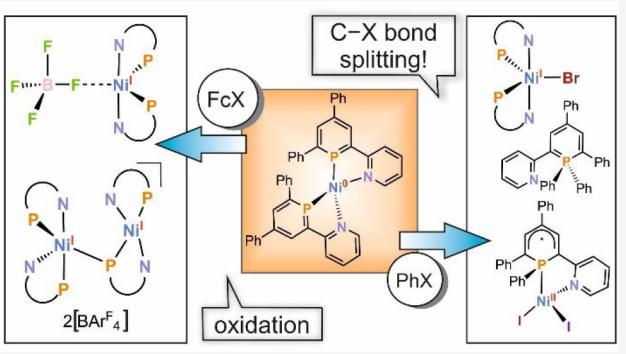

INTRODUCTION

Nickel(0) complexes have become ubiquitous in homogeneous catalysis and are used for a wide range of processes,[1] including alkene and alkyne oligomerization reactions,[2−7] as well as Kumada-type cross couplings.[8] The complex bis(2,2′-bipyridine)nickel(0) (**A**; Figure 1) is an archetypal example of a Ni(0) species with versatile catalytic properties and has found diverse applications in various (electro)chemical reactions and catalysis.[9−13]

Replacing the pyridyl moieties in **A** with valence isoelectronic phosphinine (also referred to as phosphabenzene) units can have a significant impact on both the electronic structure and reactivity of the corresponding coordination compound.[14−18] Considering the versatile applications of **A** and bipyridine complexes, as well as the fact that monophosphininenickel(0) complexes are well-investigated,[19−24] it is quite surprising that phosphorus-containing analogues of **A** are extremely rare.[25] In fact, the known examples appear to be limited to just a single species described by Le Floch and coworkers, who reported that reactions of 2,2′-(4,5-dimethyl)-biphosphinine[26] with nickel(0) sources, such as Ni(cod)$_2$ (cod = 1,5-cyclooctadiene), afford the homoleptic bis(biphosphinine) complex **B** (Figure 1).[27] However, the reactivity of this complex—and almost all related chelating phosphininenickel complexes—remains unexplored.[28,29]

We have recently become interested in the coordination chemistry of the donor-functionalized phosphinine 2-(2′-pyridyl)-4,6-diphenylphosphinine (**L**), a "hybrid" P,N ligand that can be considered to be a cross between previously explored biphosphinines and the ubiquitous bipyridines.[30−32] **L** possesses two electronically distinct binding sites—a "soft" P and a "hard" N donor site—which can have a significant impact on its coordination properties and reactivity. Although a large variety of 4d and 5d transition-metal complexes of **L** have been prepared, syntheses of 3d metal complexes remain scarce.[33−41] Nevertheless, we have recently demonstrated that the combination of a late 3d metal with ligand **L** can lead to versatile coordination chemistry and, even more importantly, to useful reactivity, as exemplified by the facile cleavage of one C═O bond in CO$_2$ by the Fe complex **C** (Figure 1).[42]

EXPERIMENTAL DETAILS

All experiments were performed under an atmosphere of dry argon using standard glovebox and Schlenk-line techniques. Tetrahydrofur-

Received: April 16, 2020
Published: July 2, 2020

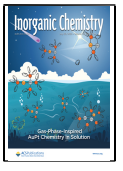

https://dx.doi.org/10.1021/acs.inorgchem.0c01115
Inorg. Chem. 2020, 59, 9951−9961

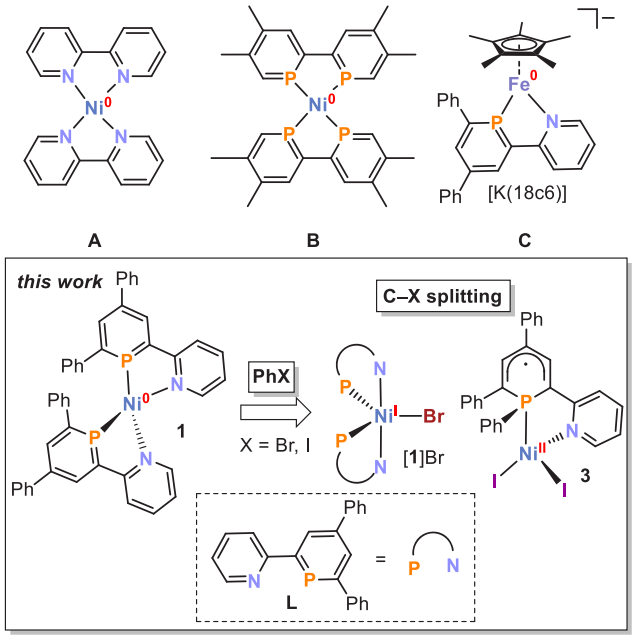

Figure 1. Previously reported bidentate, chelated phosphinine-containing transition-metal complexes (**A**–**C**) and the new nickel pyridylphosphinine complexes (**1**, [**1**]Br, and **3**) described herein. 18c6 = [18]crown-6.

an (THF), toluene, diethyl ether, and *n*-hexane were purified, dried, and degassed using an MBraun SPS800 solvent purification system. Benzene was distilled and degassed with Schlenk techniques. Deuterated THF and benzene were purchased from Sigma-Aldrich and used as received. Bromobenzene and iodobenzene were purchased from Sigma-Aldrich and used as received. [(IPr)Ni-(H_2C═$CHSiMe_3$)$_2$] [**D**;[43] IPr = 1,3-bis(2,6-diisopropylphenyl)-imidazolin-2-ylidene], 2-(2′-pyridyl)-4,6-diphenylphosphinine (**L**),[30] $FcBF_4$,[44] $FcPF_6$,[45] and $FcBAr^F{}_4$[44] (Fc = ferrocenyl; $BAr^F{}_4^-$ = [B{3,5-$(CF_3)_2C_6H_3$}$_4$]$^-$) were synthesized according to literature procedures.

NMR spectra were recorded on Bruker Avance 400 spectrometers at 300 K. ^{1}H and ^{13}C{^{1}H} NMR spectra were referenced internally to residual solvent resonances, while ^{31}P{^{1}H} and ^{31}P NMR spectra were referenced externally to 85% H_3PO_4(aq). The assignment of ^{1}H and ^{13}C NMR signals was confirmed by two-dimensional (COSY, HSQC, and HMBC) experiments.

Magnetic susceptibilities in solution were determined by the Evans NMR method in THF-d_8 at room temperature. UV–vis spectra were recorded using a Varian Cary 50 spectrometer. Elemental analyses were determined by the analytical department of the University of Regensburg. Cyclic voltammograms were recorded with a CH Instruments electrochemical analyzer. Gas chromatography with a flame ionization detector (GC-FID): Shimadzu GC2010plus. Carrier gas: H_2. Column: Restek Rxi (30 m × 0.25 mm × 0.25 μm) Carrier gas: H_2. Standard heating procedure: 50 °C (2 min), 25 °C·min^{-1} → 280 °C (5 min). Gas chromatography-mass spectrometry (GC-MS) HP6890 system with a 7683B injector and an Agilent 7820A system. Column: HP-5, 19091J-413 (30 m × 0.32 mm × 0.25 μm). Carrier gas: N_2. Calibration of substrates and products with internal standard *n*-pentadecane and analytically pure samples. The experimental X-band electron paramagnetic resonance (EPR) spectra were recorded on a Bruker EMX spectrometer (Bruker BioSpin Rheinstetten) equipped with a He temperature-controlled cryostat system (Oxford Instruments). The *g* values were calculated with the *ORCA* software package at the B3LYP/def2-TZVP level of theory. The spectrum was analyzed and simulated using the *W95EPR* program of Prof. Frank Neese.

Single-crystal X-ray diffraction (XRD) data were recorded on an Agilent Technologies SuperNova diffractometer with Cu Kα radiation (λ = 1.54184 Å). Either semiempirical multiscan absorption corrections[46] or analytical ones[47] were applied to the data. The structures were solved with *SHELXT*,[48] and least-squares refinements on F^2 were carried out with *SHELXL*.[49] The H atoms were located in idealized positions and refined isotropically with a riding model. CCDC 2007973 (for [Ni(2-Py-4,6-Ph_2-PC_5H_2)$_2$] (**1**)), 1988434 (for [**1**]BF_4), 1988435 (for [**1**(THF)]PF_6), 1988436 (for [$\mathbf{1}_2$]($BAr^F{}_4$)$_2$), 1988437 (for **2**), 1988438 (for [**1**]Br), and 1988439 (for **3**) contain the supplementary crystallographic data for this paper. These data can be obtained free of charge from the Cambridge Crystallographic Data Centre. The selected crystal of **1a** was a nonmerohedral twin. The twin law was determined with the *CrysAlisPro* software (Rigaku Oxford Diffraction, 2019). Component 2 rotated by −179.7003° around [−0.71, 0.71, −0.01] in reciprocal space or [−0.77, 0.64, 0.03] in direct space. The structure was refined with the corresponding *HKLF5* file (see the Supporting Information for further details). For compound [**1**]Br, a solvent mask was calculated, and 40 electrons were found in a volume of 160 Å in one void per unit cell. This is consistent with the presence of 0.5 equiv of THF per asymmetric unit, which accounts for 40 electrons per unit cell. A checkcif report (http://checkcif.iucr.org/) for [$\mathbf{1}_2$]($BAr^F{}_4$)$_2$ shows a level B alert [PLAT910_ALERT_3_B: Missing # of FCF Reflection(s) Below Theta(Min)]. This alert was introduced during data collection and cannot be corrected by refinement. However, it will not affect the validity of the refined structure.

Synthesis. *Synthesis of 1.* Compound **1** was prepared in an MBraun argon glovebox. **1** is sensitive toward moisture and air. **1** is soluble and stable in benzene, THF, and toluene. A solution of **L** (2.5 equiv, 125 mg, 0.385 mmol) in benzene (2 mL) was added dropwise to a solution of **D** (1 equiv, 100 mg, 0.154 mmol) in benzene at room temperature. An immediate color change from yellow to deep purple was observed. The reaction mixture was stirred for 16 h at room temperature. Volatiles were completely removed, and the deep-purple residue was washed with *n*-hexane (3 × 2 mL) in order to remove IPr. The remaining residue was extracted with benzene (4 × 2 mL) and layered with *n*-hexane (12 mL). **1** was isolated as deep-purple crystals after decanting the mother liquor, washing with *n*-hexane (3 × 2 mL), and drying under vacuum. Crystals suitable for single-crystal XRD were grown from the slow diffusion of *n*-hexane into a benzene solution of **1**. Yield: 40 mg, 37%. Elem anal. Calcd for $C_{44}H_{32}N_2P_2Ni$ (M_w = 709.39 g·mol^{-1}): C, 74.50; H, 4.55; N, 3.95. Found: C, 74.98; H, 4.70; N, 3.77. UV–vis [THF; λ_{max}/nm (ε_{max}/L·mol^{-1}·cm^{-1})]: 290 (98632), 520 (27940), 816 (20814). ^{1}H NMR (400.13 MHz, 300 K, THF-d_8): δ 7.05–7.11 (m, 6H, H of C^{2,4}–*Ph*), 7.18–7.21 (m, 2H, H of NC_5H_4), 7.33–7.37 (m, 2H, H of C^{2,4}–*Ph*), 7.41–7.45 (m, 4H, H of C^{2,4}–*Ph*), 7.79–7.81 (m, 4H, H of C^{2,4}–*Ph*), 7.85–7.86 (m, 2H, H of NC_5H_4), 7.90 (d, 4H, H of C^{2,4}–*Ph*, J_{HH} = 7 Hz), 8.30 (pt, 2H, $H^{3,5}$ of $PC_5H_2Ph_2Py$, $^4J_{HH}$ = 5 Hz), 8.43 (d, 2H, H of NC_5H_4, J_{HH} = 8 Hz), 8.55 (pt, 2H, $H^{3,5}$ of $PC_5H_2Ph_2Py$, $^4J_{HH}$ = 5 Hz), 8.86 (d, 2H, H of NC_5H_4, J_{HH} = 5 Hz). ^{13}C{^{1}H} NMR (100.61 MHz, 300 K, THF-d_8): δ 119.3 (s, *C* of NC_5H_4), 122.5 (s, *C* of NC_5H_4), 126.7 (s, *C* of C^{2,4}–*Ph*), 126.8 (s, *C* of C^{2,4}–*Ph*), 127.0 (s, *C* of C^{2,4}–*Ph*), 127.4 (t, 7 Hz), 129.0 (s, *C* of C^{2,4}–*Ph*), 129.6 (s, *C* of C^{2,4}–*Ph*), 131.4 (s, *C* of C^{2,4}–*Ph*), 133.7 (m, *C* of NC_5H_4), 137.4 (t, *C* of C^{2,4}–*Ph*, *J* = 7 Hz), 143.2 (m, *C* of $PC_5H_2Ph_2Py$), 143.9 (m, *C* of $PC_5H_2Ph_2Py$), 145.1 (m, *C* of $PC_5H_2Ph_2Py$), 146.6 (m, *C* of $PC_5H_2Ph_2Py$), 153.1 (m, *C* of NC_5H_4). ^{31}P{^{1}H} NMR (161.98 MHz, 300 K, THF-d_8): δ 179.4. ^{31}P NMR (161.98 MHz, 300 K, THF-d_8): δ 179.4.

Synthesis of [1]BF_4. Compound [**1**]BF_4 was prepared in an MBraun argon glovebox. [**1**]BF_4 is sensitive toward moisture and air. [**1**]BF_4 is soluble and stable in benzene, THF, and toluene. **1** (50 mg, 0.07 mmol) was dissolved in THF (1 mL), and $FcBF_4$ (12 mg, 0.07 mmol) was added at room temperature. An immediate color change from deep purple to brown was observed. The color changed further to green-brown upon stirring overnight. The solvent of the green reaction mixture was completely removed, and ferrocene was removed by sublimation under high vacuum (50 °C, ca. 10^{-5} mbar). The remaining brown residue was extracted with THF (2 mL) and layered with *n*-hexane (4 mL). After crystallization for 2 days at −35 °C, [**1**]BF_4 could be isolated as a brown powder. Crystals suitable for single-crystal XRD were grown from the slow diffusion of *n*-hexane

https://dx.doi.org/10.1021/acs.inorgchem.0c01115
Inorg. Chem. 2020, 59, 9951–9961

into a toluene solution of [**1**]BF_4. Yield: 43 mg, 77%. Elem anal. Calcd for $C_{44}H_{32}N_2P_2NiBF_4$ (M_w = 796.20 g·mol^{-1}): C, 66.38; H, 4.05; N, 3.52. Found: C, 65.17; H, 4.26; N, 3.35. UV−vis [THF; λ_{max}/nm (ε_{max}/L·mol^{-1}·cm^{-1})]: 284 (38665), 338 (sh, 15363), 466 (8545). μ_{eff} (THF-d_8): 2.0(1) μ_B.

Synthesis of [1(THF)]PF_6. Compound [**1**(THF)]PF_6 was prepared in an MBraun argon glovebox. [**1**(THF)]PF_6 is sensitive toward moisture and air. [**1**(THF)]PF_6 is soluble and stable in benzene, THF, and toluene. **1** (50 mg, 0.07 mmol) was dissolved in THF (1 mL), and $FcPF_6$ (23 mg, 0.07 mmol) was added at room temperature. A slow color change from deep purple to brown green was observed. The color changed further to deep brown upon stirring overnight. The solvent of the brown reaction mixture was completely removed, and ferrocene was removed by sublimation under high vacuum (50 °C, ca. 10^{-5} mbar). The remaining brown residue was extracted with THF (2 mL) and layered with *n*-hexane (6 mL). After crystallization for 1 day at −35 °C, [**1**(THF)]PF_6 could be isolated as a deep-brown powder. Crystals suitable for single-crystal XRD were grown from the slow diffusion of *n*-hexane into a THF solution of [**1**(THF)]PF_6. Yield: 53 mg, 88%. Elem anal. Calcd for $C_{44}H_{32}N_2P_3NiF_6(C_4H_8O)$ (M_w = 926.47 g·mol^{-1}): C, 62.23; H, 4.35; N, 3.02. Found: C, 62.12; H, 4.41; N, 2.93. UV−vis [toluene; λ_{max}/nm (ε_{max}/L·mol^{-1}·cm^{-1})]: 334 (sh, 6649), 450 (2617), 659 (1805). μ_{eff} (THF-d_8): 1.7(1) μ_B.

Synthesis of [1_2](BAr^F_4)$_2$. Compound [$\mathbf{1}_2$](BAr^F_4)$_2$ was prepared in an MBraun argon glovebox. [$\mathbf{1}_2$](BAr^F_4)$_2$ is sensitive toward moisture and air. [$\mathbf{1}_2$](BAr^F_4)$_2$ is soluble and stable in diethyl ether, benzene, THF, and toluene. **1** (50 mg, 0.07 mmol) and $FcBAr^F_4$ (74 mg, 0.07 mmol) were dissolved in THF (2 mL) at room temperature. An immediate color change from deep purple to brown was observed. After stirring overnight, the solution turned green, and the solvent of the reaction mixture was completely removed. Ferrocene was removed by washing with *n*-hexane (3 × 2 mL). The remaining oily green residue was extracted in diethyl ether (2 mL) and layered with *n*-hexane (6 mL). [$\mathbf{1}_2$](BAr^F_4)$_2$ was isolated as a dark-brown powder after crystallization at −35 °C for 2 days. Crystals suitable for X-ray crystallography were obtained by the slow diffusion of *n*-hexane into a diethyl ether solution of [$\mathbf{1}_2$](BAr^F_4)$_2$. Ether solutions of [$\mathbf{1}_2$](BAr^F_4)$_2$ show a green color, while ether-free [$\mathbf{1}_2$](BAr^F_4)$_2$ appears brown. Crystals suitable for single-crystal XRD were grown from the slow diffusion of *n*-hexane into a diethyl ether solution of [$\mathbf{1}_2$](BAr^F_4)$_2$. Yield: 86 mg, 78%. Elem anal. Calcd for $C_{151}H_{88}B_2F_{48}N_4Ni_2P_4$ (M_w = 3130.41 g·mol^{-1}): C, 57.88; H, 2.83; N, 1.79. Found: C, 58.48; H, 3.21; N, 1.58. UV−vis [diethyl ether; λ_{max}/nm (ε_{max}/L·mol^{-1}·cm^{-1})]: 279 (55432), 330 (sh, 22957), 454 (8288), 635 (4397). UV−vis [toluene; λ_{max}/nm (ε_{max}/L·mol^{-1}·cm^{-1})]: 330 (sh, 19450), 416 (6438), 505 (5831). μ_{eff} (THF-d_8): 1.7(1) μ_B.

Synthesis of 2 and [1]Br. Compounds **2** and [**1**]Br were prepared in an MBraun argon glovebox. [**1**]Br is sensitive toward moisture and air. [**1**]Br is soluble and stable in benzene, THF, and toluene. **2** is soluble and stable in *n*-hexane. Bromobenzene (7.5 μL, 0.07 mmol) was added to a solution of **1** (50 mg, 0.07 mmol) in benzene (1 mL), and this reaction mixture was heated to 60 °C overnight. The deep-purple solution turned deep red upon heating. The mixture was cooled to room temperature and layered with *n*-hexane (5 mL). After crystallization at room temperature over 2 days, a deep-red solid was isolated by decanting the fluorescent pink solution. After washing with *n*-hexane (2 × 2 mL) and drying under vacuum, [**1**]Br was isolated as a deep-red powder. Crystals suitable for single-crystal XRD were grown from the slow diffusion of *n*-hexane into a THF solution of [**1**]Br. Yield: 25 mg, 45%. Elem anal. Calcd for $C_{44}H_{32}BrN_2P_2Ni$ (M_w = 789.30 g·mol^{-1}): C, 66.96; H, 4.09; N, 3.55. Found: C, 64.83; H, 4.27; N, 3.33. UV−vis [THF; λ_{max}/nm (ε_{max}/L·mol^{-1}·cm^{-1})]: 280 (35690), 480 (6780). μ_{eff} (THF-d_8): 2.1(1) μ_B. The decanted fluorescent pink solution was evaporated to dryness, and the remaining pink residue was extracted with *n*-hexane (3 × 2 mL). Slow evaporation at room temperature gave pure **2** as a pink powder. Crystals suitable for single-crystal XRD were grown from the slow evaporation of a *n*-hexane solution of **2**. Yield: 5 mg, 15%. Elem anal. Calcd for $C_{34}H_{26}NP$ (M_w = 479.56 g·mol^{-1}): C, 85.16; H, 5.46; N, 2.92. Found: C, 84.34; H, 5.37; N, 2.70. UV−vis [*n*-hexane; λ_{max}/nm (ε_{max}/L·mol^{-1}·cm^{-1})]: 265 (6456), 300 (8900), 333 (8933), 516 (8023). ^{1}H NMR (400.13 MHz, 300 K, C_6D_6): δ 6.21−6.25 (m, 1H, H of $C^{3,5}$ of $PC_5H_2Ph_2Py$), 6.86−7.00 (m, 10H, $H_{aromatic}$), 7.08−7.12 (m, 2H, $H_{aromatic}$), 7.21−7.23 (m, 1H, $H_{aromatic}$), 7.32−7.36 (m, 2H, $H_{aromatic}$), 7.81−7.82 (m, 1H, H of $C^{3,5}$ of $PC_5H_2Ph_2Py$), 7.91−7.97 (m, 4H, $H_{aromatic}$), 8.11−8.20 (m, 1H, $H_{aromatic}$), 8.11−8.20 (dd, 1H, H of pyridyl group, J_{HH} = 32 Hz, J_{PH} = 2 Hz). $^{13}C\{^1H\}$ NMR (100.61 MHz, 300 K, C_6D_6): δ 80.1 (s), 81.1 (s), 94.7 (s), 95.6 (s), 112.8 (s), 112.9 (s), 115.9 (d, *J* = 9 Hz), 116.3 (s), 123.9 (s), 124.7 (s), 125.7 (s), 128.3 (s), 128.6 (s), 129.2 (s), 129.5 (d, *J* = 5 Hz), 130.1 (s), 130.2 (d, *J* = 3 Hz), 132.6 (s), 132.7 (s), 133.4 (d, *J* = 10 Hz), 135.3 (s), 141.4 (s), 141,47 (s), 141.52 (s), 143.7 (s), 146.6 (s), 158.6 (s). $^{31}P\{^1H\}$ NMR (161.98 MHz, 300 K, C_6D_6): δ 4.7(s). ^{31}P NMR (161.98 MHz, 300 K, C_6D_6): δ 4.7 (m). The reaction with 2 equiv of bromobenzene (0.14 mmol, 15 μL) with 1 equiv of **1** (50 mg, 0.07 mmol) afforded [**1**]Br (42 mg, 75%) and **2** (10 mg, 30%) in higher yields.

Synthesis of 2 and 3. Compounds **2** and **3** were prepared in an MBraun argon glovebox. **3** is sensitive toward moisture and air. **3** is soluble and stable in benzene, THF, and toluene. **2** is soluble and stable in *n*-hexane. Iodobenzene (8 μL, 0.07 mmol) was added to a solution of **1** (50 mg, 0.07 mmol) in toluene (1 mL), and this reaction mixture was heated to 60 °C overnight. The deep-purple solution turned deep red upon heating. The mixture was cooled to room temperature and layered with *n*-hexane (8 mL). After crystallization at room temperature overnight, a deep-green solid was isolated by decanting the fluorescent pink solution. After washing with *n*-hexane (2 × 2 mL) and drying under vacuum, **3** was isolated as a deep-green powder. Crystals suitable for single-crystal XRD were grown from the slow diffusion of *n*-hexane into a toluene solution of **3**. Yield: 38 mg (64%). Elem anal. Calcd for $C_{28}H_{21}I_2NPNi·(C_7H_8)_{1.4}$ (M_w = 843.96 g·mol^{-1}): C, 53.80; H, 3.85; N, 1.66. Found: C, 53.99; H, 3.58; N, 1.98. UV−vis [THF; λ_{max}/nm (ε_{max}/L·mol^{-1}·cm^{-1})]: 285 (24370), 450 (4788), 614 (2600). μ_{eff} (THF-d_8): 3.2(1) μ_B. The decanted fluorescent pink solution was evaporated to dryness, and the remaining pink residue was extracted with *n*-hexane (3 × 2 mL). Slow evaporation at room temperature gave pure **2** as a pink powder. Yield: 10 mg, 30%.

RESULTS AND DISCUSSION

Encouraged by our previous results with Fe, we were motivated to investigate the coordination compounds of the pyridylphosphinine ligand **L** with other late 3d metals. Given the paucity of prior Ni complexes containing chelating phosphinine ligands—and, in particular, the lack of corresponding reactivity studies—we were specifically motivated to study the reactivity of **L** toward suitable low-valent Ni sources and decided to start with the formal Ni(0) source **D**.[43] While the 1:1 reaction of **D** and **L** resulted in a mixture of several inseparable products (Figure S11), the reaction of **D** with 2.5 equiv of **L** led to the selective formation of a single phosphorus-containing species (**1**), characterized by a singlet in the $^{31}P\{^1H\}$ NMR spectrum at δ = 179.4 ppm (Scheme 1; for the spectrum, see Figure S5). Isolation of **1** was achieved by the removal of volatiles (including $H_2C{=}CHSiMe_3$) under vacuum, the removal of IPr by washing with *n*-hexane, and the layering of a purple solution of **1** in benzene with *n*-hexane at room temperature for 2 days, to afford a pure, crystalline material in 35% yield.

Compound **1** was fully characterized by NMR and UV−vis spectroscopy, elemental analysis, and cyclic voltammetry (CV; see the Supporting Information, SI). The collected data are all consistent with the formulation of **1** as the 1:2 homoleptic chelate complex [Ni(**L**)$_2$] (Scheme 1), which is also in line with the reaction stoichiometry employed.

https://dx.doi.org/10.1021/acs.inorgchem.0c01115
Inorg. Chem. 2020, 59, 9951−9961

Scheme 1. Synthesis of 1 Using D as a Ni(0) Precursor[a]

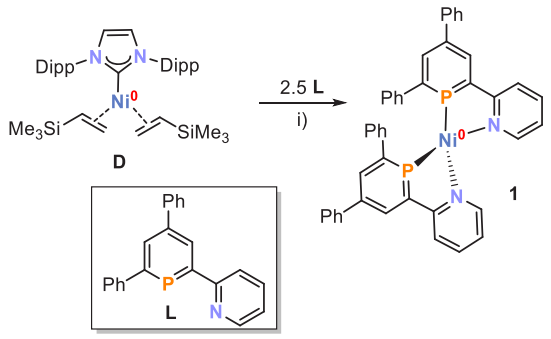

[a](i) C_6H_6, 25 °C, 16 h; Dipp = 2,6-diisopropylphenyl.

Single crystals suitable for XRD could be obtained by the slow diffusion of *n*-hexane into a solution of **1** in benzene. As anticipated, the solid-state molecular structure shows the expected homoleptic chelate complex, where the Ni center is coordinated by two 2-(2′-pyridyl)phosphinine ligands **L** (Figure 2). This leads to a distorted tetrahedral coordination

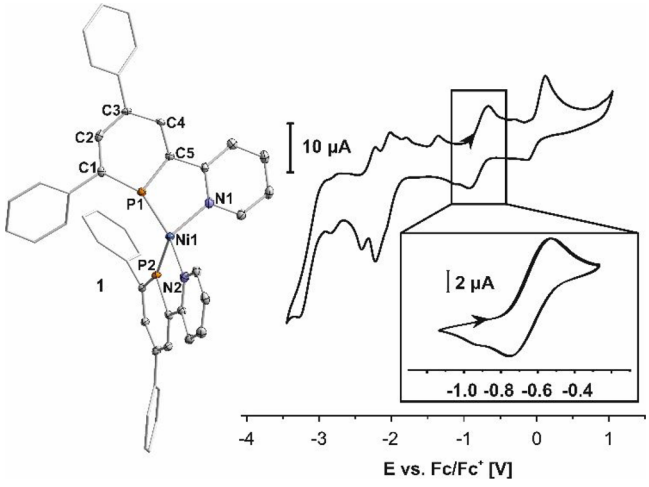

Figure 2. Molecular structure of **1** in the solid state (left). Ellipsoids are drawn at the 40% probability level; H atoms are omitted for clarity; four phenyl groups are displayed in wireframe for clarity. Selected bond lengths [Å] and bond angles [deg]: Ni1−N1 2.005(6), Ni1−N2 1.998(6), Ni1−P1 2.091(2), Ni1−P2 2.092(2); P1−Ni1−P2 128.15(8), N1−Ni1−N2 110.4(2), P1−Ni1−N2 124.67(18), N1−Ni1−P2 129.03(17), P1−Ni1−N1 84.05(17), P2−Ni1−N2 84.28(17), C1−P1−C5 102.2(3), C1′−P2−C5′ 102.0(3). Cyclic voltammograms of **1** (right; from *E* (V) = −3.4 to +1.1 and from *E* (V) = −1.1 to −0.2; scan rate 100 mV).

Table 1. Geometry Indices (τ_4 and τ_5)[55,56] and Magnetic Moments (μ_{eff}, THF-d_8, 300 K) of Reported Ni Complexes

compound	τ_4	τ_5	μ_{eff}
1	0.80		
[**1**]BF_4		0.53	2.0(1)
[**1**(THF)]PF_6		0.71	1.7(1)
[**1**]Br		0.79	2.1(1)
3	0.95		3.2(1)

sphere around the Ni center (the calculated geometry index for **1** is τ_4 = 0.80; see Table 1; cf. τ_4 = 0 and 1 for the ideal square-planar and tetrahedral geometries, respectively). The P−Ni−N bite angles are 84.05(17)° for P1−Ni1−N1 and 84.28(17)° for P2−Ni1−N2. The C1−P1−C5 angle of **1** is approximately 102°, close to the one in free phosphinines (ca. 100°). This is in line with earlier observations that electron-rich metal fragments cause only a marginal opening of the C1−P1−C5 angle in the coordinated phosphinine. In contrast, this effect is much more pronounced in coordination compounds, in which the phosphinine ligand is bound to more electron-poor metal centers with reduced π-back-donation ability. Those complexes are usually characterized by a high reactivity of the P═C double bond toward nucleophilic attack.[31,50−52]

Complex **1** is the first example of a Ni complex containing a pyridylphosphinine ligand. The molecular structure of **1** is reminiscent of ubiquitous 2,2′-bipyridinenickel(0)[53] complexes, which are known for their versatile redox properties and corresponding utilization in the electrochemical reduction of aryl halides, for example.[9−11,54] Thus, in order to determine the redox properties of **1**, cyclic voltammograms were recorded in THF using [nBu$_4$N]PF_6 as a supporting electrolyte. Several irreversible and quasi-reversible oxidation and reduction processes are apparent (Figure 2). However, perhaps the most interesting process is the quasi-reversible oxidation observed at $E_{1/2}$ = −0.6 V versus Fc/Fc$^+$. Because this feature is well-behaved on the CV time scale, it was anticipated that **1** might also be oxidized in a preparative manner using a suitable chemical oxidant. Thus, **1** was treated with several different ferrocenium salts FcX [Fc = ferrocenium; X = BF_4, PF_6, and $BAr^F{}_4$, where Ar^F = 3,5-$(CF_3)_2C_6H_3$] in order to obtain the corresponding cationic Ni complexes [**1**]BF_4, [**1**(THF)]PF_6, and [$\mathbf{1}_2$]$(BAr^F{}_4)_2$ (Scheme 2), which could all be characterized crystallographically.

Scheme 2. Synthesis of Ni(I) Complexes [1]BF_4 (77% Isolated Yield), [1(THF)]PF_6 (88%), and [$\mathbf{1}_2$]$(BAr^F{}_4)_2$ (78%) via the Reaction of 1 with Ferrocenium Salts in THF at 25 °C

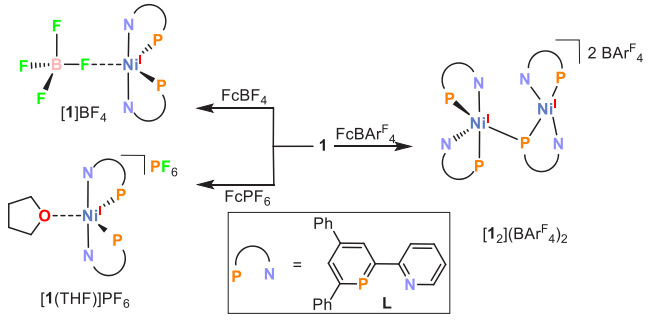

The solid-state molecular structures of [**1**]BF_4 and [**1**(THF)]PF_6 reveal a common structural motif: trigonal-bipyramidal Ni(I) complexes coordinated by two ligands **L** and direct equatorial coordination of an additional ligand (Figure 3). In [**1**]BF_4, the tetrafluoroborate anion shows an interaction of one F atom with the metal center [Ni1−F1 distance: 2.2729(9) Å]. The value of the geometry index for [**1**]BF_4 (τ_5 = 0.53) is between those expected for square-pyramidal (τ_5 = 0) and trigonal-bipyramidal (τ_5 = 1; Table 1) complexes. For [**1**(THF)]PF_6, the fifth coordination site at Ni is occupied by a THF solvent molecule [Ni1−O1 2.1355(15) Å], rather than by the counteranion, which can be attributed to the reduced donor strength of the PF_6^- anion relative to BF_4^- (Figure 3). A similar coordination motif was observed following the

https://dx.doi.org/10.1021/acs.inorgchem.0c01115
Inorg. Chem. 2020, 59, 9951−9961

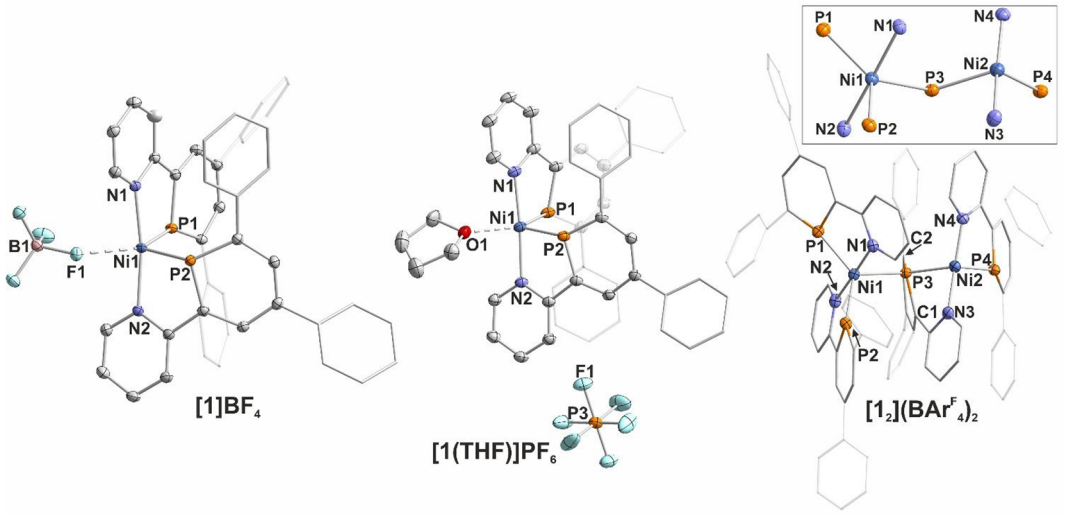

Figure 3. Solid-state molecular structures of $[\mathbf{1}]BF_4$, $[\mathbf{1}(THF)]PF_6$, and $[\mathbf{1}_2](BAr^F{}_4)_2$. Ellipsoids are drawn at the 40% probability level; H atoms are omitted for clarity; some phenyl groups are displayed in wireframe and are transparent for clarity. For $[\mathbf{1}]BF_4$, a toluene solvent molecule is omitted for clarity. Selected bond lengths [Å] and bond angles [deg]: Ni1−P1 2.2328(4), Ni1−P2 2.2147(4), Ni1−N1 2.0449(12), Ni1−N2 2.0340(12), Ni1−F1 2.2729(9), P1−C1 1.7422(15), C1−C2 1.397(2), C2−C3 1.404(2), C3−C4 1.402(2), C4−C5 1.391(2), P1−C5 1.7409(14); C1−P1−C5 102.92(7), P1−Ni1−P2 108.070(16), P1−Ni1−F1 114.04(3), F1−Ni1−P2 137.73(3), P2−Ni1−N2 82.66(4), P1−Ni1−N1 82.92(4). For $[\mathbf{1}(THF)]PF_6$, one THF molecule, which is not coordinated to the complex, was omitted for clarity. Selected bond lengths [Å] and bond angles [deg]: Ni1−P1 2.1871(6), Ni1−P2 2.1857(6), Ni1−N1 2.0611(16), Ni1−N2 2.0586(17), Ni1−O1 2.1355(15), P1−C1 1.734(2), C1−C2 1.389(3), C2−C3 1.407(3), C3−C4 1.396(3), C4−C5 1.387(3), P1−C5 1.738(2); C1−P1−C5 103.42(10), P1−Ni1−P2 103.59(2), P1−Ni1−O1 133.20(4), O1−Ni1−P2 123.20(4), P2−Ni1−N2 81.92(5), P1−Ni1−N1 81.91(5). For $[\mathbf{1}_2](BAr^F{}_4)_2$, two $BAr^F{}_4{}^-$ anions and a *n*-hexane solvent molecule were omitted for clarity. The crystal of $[\mathbf{1}_2](BAr^F{}_4)_2$ contained a second crystallographically independent molecule with very similar structural parameters, and only one of these molecules is shown. The structure of the metal core of $[\mathbf{1}_2](BAr^F{}_4)_2$ is shown in the inset. Selected bond lengths [Å] and bond angles [deg]: Ni1−N1 2.059(3), Ni1−N2 2.091(3), Ni1−P1 2.2275(11), Ni1−P2 2.2531(11), Ni1−P3 2.4071(11), Ni2−N3 1.968(4), Ni2−N4 1.960(4), Ni2−P3 2.2692(11), Ni2−P4 2.2360(13); Ni1−P3−Ni2 125.9074 (10), P1−Ni1−N1 80.6936(11), P2−Ni1−N2 82.1127(13), P3−Ni2−N3 85.8814(12), P4−Ni2−N4 83.9324(11).

electrophilic addition of Ph_3SnCl to anionic homoleptic biphosphininecobalt and -rhodium complexes, as described by Le Floch and co-workers.[17]

The magnetic moments of $[\mathbf{1}]BF_4$ and $[\mathbf{1}(THF)]PF_6$ [2.0(1) and 1.7(1) μ_B, respectively, in THF-d_8 at 300 K] were determined by the Evans NMR method and are consistent with $S = {}^1/_2$ Ni(I) centers (Table 1). EPR measurements of $[\mathbf{1}]BF_4$ and $[\mathbf{1}(THF)]PF_6$ were recorded in toluene glasses at 20 and 40 K, respectively, and also confirm the presence of a single unpaired electron at each Ni center (for full details, see the SI). The EPR signal of $[\mathbf{1}]BF_4$ appears almost isotropic because of the broad and overlapping signals of the **g** tensor. However, it is better described as a rhombic system, which is indicated by the asymmetric shape of the signal. The observed **g** tensor with the simulated principal components g_{11} = 2.195, g_{22} = 2.127, and g_{33} = 2.060 is consistent with a Ni-centered radical in a system with small *g* anisotropy (for the spectrum, see Figure S20). The EPR spectrum of $[\mathbf{1}(THF)]PF_6$ displays similarly overlapping signals of the **g** tensor and can again be described as a rhombic system with small *g* anisotropy. Poorly resolved hyperfine interactions were observed on (at least) one **g** tensor, and satisfactory simulation was achieved after the inclusion of hyperfine coupling (135 and 150 MHz) to ^{31}P ($I = {}^1/_2$) on two **g** tensors. The observed **g** tensor (simulated **g** tensor: g_{11} = 2.200, g_{22} = 2.129, and g_{33} = 2.035) is again consistent with a Ni-centered radical (for the spectrum, see Figure S21). These results are consistent with the density functional theory (DFT) calculations carried out on $[\mathbf{1}]BF_4$, which show a large amount of spin density on Ni (0.85) and reproduce the experimental **g** tensor quite well [TPSSh/IGLO-III+CP(PPP); see the SI].

The reaction of **1** with $FcBAr^F{}_4$ leads to a product with a notably different structure, at least in the solid state. In this case, the product $[\mathbf{1}_2](BAr^F{}_4)_2$ is formed, which crystallizes as a dicationic dinuclear Ni complex fragment with two Ni(I) centers bridged by one P atom of one phosphinine ligand **L**. The charge of the dication is balanced by two $BAr^F{}_4{}^-$ anions, which show no close contacts with either Ni center (Figure 3). Compound $[\mathbf{1}_2](BAr^F{}_4)_2$ is a rare example of a complex in which the phosphinine ligand shows a μ_2-P bridging coordination mode.[57−65] The corresponding bipyridine μ_2-N bridging mode is even scarcer (despite the fact that these complexes were studied far more extensively) because of the reduced electronic versatility of the lighter heterocycle.[66−68] The Ni−N and Ni−P distances in $[\mathbf{1}_2](BAr^F{}_4)_2$ are similar to those in $[\mathbf{1}]BF_4$ and $[\mathbf{1}(THF)]PF_6$, except for the bridging Ni1−P3 distance, which is slightly elongated [2.4071(11) Å vs mean distance 2.246 Å], as expected for a bridging interaction. The bridging P3 atom is tetrahedrally coordinated between the two Ni(I) centers with a geometry index of τ_4 = 0.86.

Also, in contrast to $[\mathbf{1}]BF_4$ and $[\mathbf{1}(THF)]PF_6$, the EPR signal of $[\mathbf{1}_2](BAr^F{}_4)_2$ in a toluene glass at 30 K is well resolved and shows a rhombic system with small *g* anisotropy and hyperfine coupling interactions with two ^{31}P nuclei along all three **g** tensors ($A^{P1}{}_{11} = A^{P2}{}_{11}$ = 205 MHz, $A^{P1}{}_{22} = A^{P2}{}_{22}$ = 170 MHz, and $A^{P1}{}_{33} = A^{P2}{}_{33}$ = 175 MHz). The spectrum again indicates that a Ni-centered radical is present (simulated **g** tensors: g_{11} = 2.2170, g_{22} = 2.1450, and g_{33} = 2.0195; Figure S22). The found *g* values (close to 2) and well-defined

https://dx.doi.org/10.1021/acs.inorgchem.0c01115
Inorg. Chem. 2020, 59, 9951−9961

hyperfine coupling interactions are indicative for an isolated $S = {}^1/_2$ species. Thus, the EPR data might indicate that $[\mathbf{1}_2](BAr^F{}_4)_2$ dissociates in solution into two monocations $[Ni(I)\mathbf{L}_2]^+$. This is also consistent with DFT calculations on the monocation, which yield a rhombic **g** tensor ($g_z = 2.123$, $g_y = 2.116$, and $g_x = 2.015$) that is in good agreement with the experimental results.

When the EPR measurement of $[\mathbf{1}_2](BAr^F{}_4)_2$ is performed in a 2-methyltetrahydrofuran glass at 20 K instead of a toluene glass, a well-resolved rhombic system with small *g* anisotropy is again observed (Figure 4). However, in this case, additionally resolved hyperfine couplings to two equivalent ^{31}P ($I = {}^1/_2$), two equivalent ^{14}N ($I = 1$), and two equivalent ^1H ($I = {}^1/_2$) nuclei are also observed. Calculations indicate that the proton hyperfine couplings are caused by the *o*-H atoms of the pyridyl groups (see the SI for details). The simulated **g** tensor ($g_{11} = 2.2135$, $g_{22} = 2.1460$, and $g_{33} = 2.0212$) is similar to that obtained in toluene and so is again consistent with a Ni-centered radical. The presence of monocationic Ni(I) centers is additionally confirmed by the magnetic moment of 1.7(1) μ_B (in THF-d_8 at 300 K) per Ni atom measured by the Evans NMR method.

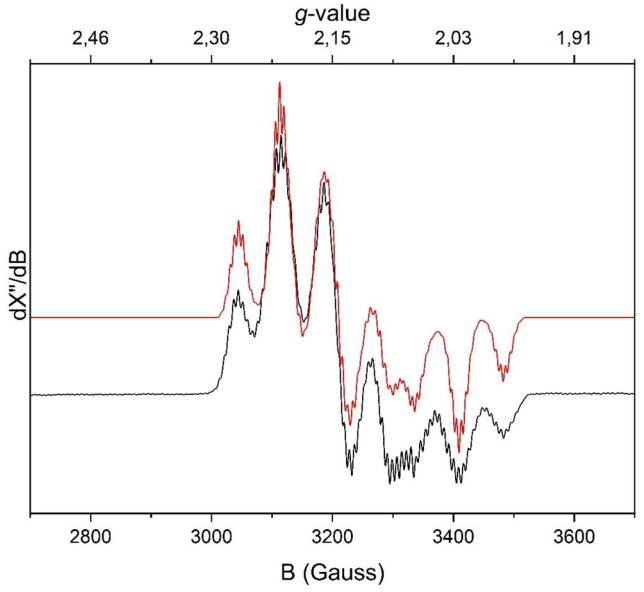

Figure 4. Experimental (black) and simulated (red) EPR spectra of $[\mathbf{1}_2](BAr^F{}_4)_2$ recorded at 20 K in a 2-methyltetrahydrofuran glass. Simulation parameters: $g_{11} = 2.2135$, $g_{22} = 2.1460$, and $g_{33} = 2.0212$; $W_{11} = 3.0$, $W_{22} = 2.5$, and $W_{33} = 3.2$; $A^{P1}{}_{11} = A^{P2}{}_{11} = 210$ MHz, $A^{P1}{}_{22} = A^{P2}{}_{22} = 212$ MHz, $A^{P1}{}_{33} = A^{P2}{}_{33} = 207$ MHz, $A^{N1}{}_{11} = A^{N}{}_{11} = 23$ MHz, $A^{N1}{}_{22} = A^{N2}{}_{22} = 28$ MHz, $A^{N1}{}_{33} = A^{N2}{}_{33} = 21$ MHz, $A^{H1}{}_{11} = A^{H2}{}_{11} = 20$ MHz, $A^{H1}{}_{22} = A^{H2}{}_{22} = 20$ MHz, and $A^{H1}{}_{33} = A^{H2}{}_{33} = 19$ MHz. Experimental conditions: microwave frequency 9.64567 GHz; power 1.589 mW; modulation amplitude 4.000 G.

In addition to simple outer-sphere oxidation, we were also interested in investigating more complex reactions of **1**, particularly given the complete lack of analogous studies for other nickel phosphinine complexes. Ni(0) complexes, in general, are very versatile and find various applications in electrochemistry and catalysis.[69,70] For example, Ni(0) species play important roles in cross-coupling reactions (e.g., Kumada reaction) because of their redox properties and ability to undergo oxidative additions with substrates such as aryl halides.[71,72] Thus, we were motivated to investigate the reactivity of **1** with the simple model cross-coupling substrates bromobenzene and iodobenzene (Scheme 3). When 1 equiv of bromobenzene was added to **1** in benzene, no change was observed at room temperature, either by eye or by $^{31}P\{^1H\}$ NMR spectroscopy. However, when the temperature was increased to 60 °C, a color change from deep purple to fluorescent red could be observed. According to GC-FID analysis, a maximum of ca. 70% bromobenzene was consumed (despite complete consumption of **1**, as indicated by $^{31}P\{^1H\}$ NMR spectroscopy) alongside the formation of a new species which shows a single $^{31}P\{^1H\}$ resonance arising as a sharp singlet at $\delta = 4.7$ ppm. This signal splits into a complex multiplet in the ^{31}P NMR spectrum. In order to characterize the corresponding species **2**, the solvent of the fluorescent red reaction mixture was completely evaporated, and the remaining residue was extracted into *n*-hexane.

Crystals of **2** were obtained by slow evaporation of the resulting fluorescent orange *n*-hexane solution. Single-crystal XRD revealed its identity as a 1,1-diphenyl-λ^5-phosphinine (Figure 5), which accounts for the observed fluorescent properties.[3073−76] This structure formally arises from the addition of two phenyl groups to the P center of the

Scheme 3. Reaction of 1 with Haloarenes PhX (X = Br, I) at 60 °C[a]

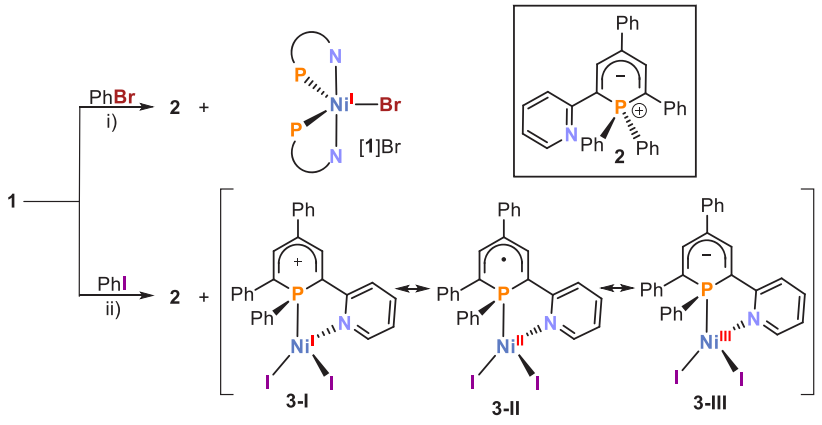

[a](i) Reaction in benzene, **2** (15% isolated yield) and [**1**]Br (45%). (ii) Reaction in toluene, **2** (30%) and **3** (64%). Possible contributions to the electronic structure of **3**, including Ni d^9 (**3-I**), Ni d^8 (**3-II**), and Ni d^7 (**3-III**) centers.

https://dx.doi.org/10.1021/acs.inorgchem.0c01115
Inorg. Chem. 2020, 59, 9951−9961

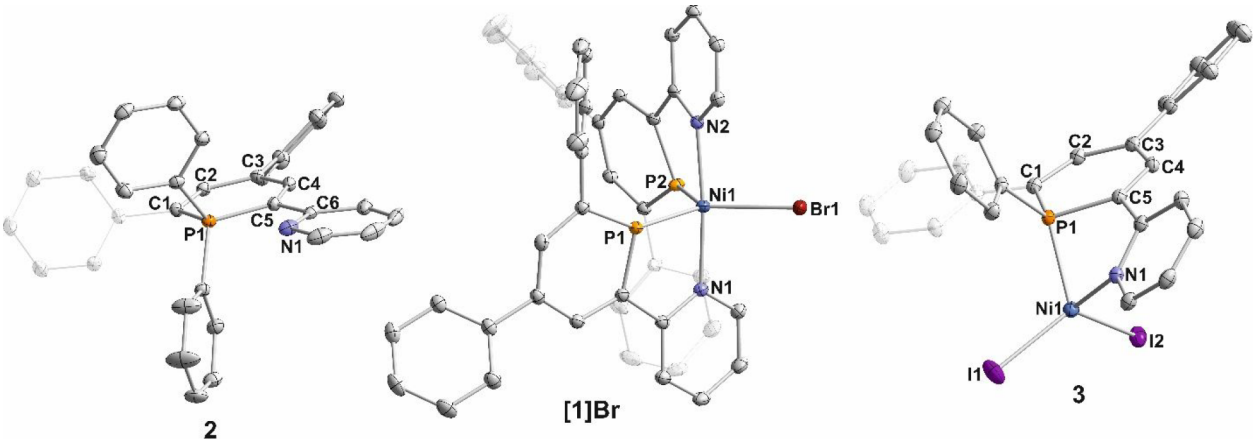

Figure 5. Solid-state molecular structures of **2**, [**1**]Br, and **3**. Ellipsoids are drawn at the 40% probability level; H atoms are omitted for clarity; some phenyl groups are transparent for clarity. Selected bond lengths [Å] and bond angles [deg] for **2**: P1−C1 1.7719(13), C1−C2 1.3724(17), C2−C3 1.4194(17), C3−C4 1.3858(18), C4−C5 1.4038(18), P1−C5 1.7553(13); C1−P1−C5 107.49(6), fold angle C1−P1−C5 1.50(8). Selected bond lengths [Å] and bond angles [deg] for [**1**]Br: Ni1−P1 2.2094(6), Ni1−P2 2.2055(6), Ni1−N1 2.1046(18), Ni1−N2 2.1045(18), Ni1−Br1 2.4889(4); P1−Ni1−P2 112.45(3), P1−Ni1−Br1 121.48(2), Br1−Ni1−P2 126.04(2), P1−Ni1−N1 80.61(4), P2−Ni1−N2 80.58(4). For **3**, toluene solvent molecule is omitted for clarity. Selected bond lengths [Å] and bond angles [deg]: Ni1−P1 2.2509(6), Ni1−I1 2.4893(4), Ni1−I2 2.5375(4), Ni1−N1 1.9941(19), P1−C1 1.774(2), C1−C2 1.387(3), C2−C3 1.414(3), C3−C4 1.417(3), C4−C5 1.370(3), P1−C5 1.779(2); C1−P1−C5 104.61(10), P1−Ni1−N1 82.59(6), I1−Ni1−I2 124.218(16), P1−Ni1−I1 116.93(2), N1−Ni1−I2 108.96(5).

phosphinine ligand **L**. As reported for other λ^5-phosphinines, the P1−C1/C5 bonds are slightly shortened compared to P−C single bonds (mean distance 1.763 Å vs sum of covalent radii 1.86 Å), while the C−C bonds are in the range of C=C double bonds (mean distance 1.395 Å vs sum of covalent radii 1.34 Å).[77] The almost planar phosphorus heterocycle is characterized by the small fold angle of 1.50(8)°, and the phenyl substituents at the P atom show bond lengths consistent with P−C single bonds (mean distance 1.817 Å).[77] Similar to the only other λ^5-pyridylphosphinine reported in the literature, the pyridyl group is essentially coplanar with the phosphinine ring [N1−C6−C5−C4 = 174.9(1)°], while the phenyl groups in 4 and 6 positions of the heterocycle are not in-plane with the central hexagon. This is in accordance with our expectations for the steric demand of the N lone pair, which is smaller than a CH group of a phenyl moiety.[76,78]

The *n*-hexane-insoluble material remaining after separation of **2** could be dissolved in THF to give a red NMR-silent solution. Single crystals suitable for XRD were obtained after layering with *n*-hexane. The molecular structure revealed the formation of a trigonal-bipyramidal Ni(I) complex, [**1**]Br, containing two **L** and one additional bromide ligand (Figure 5), in a structure very similar to those observed for [**1**]BF_4 and [**1**(THF)]PF_6. The σ bonds between the Ni center and the donor atoms of **L** (mean distances: Ni1−N 2.105 Å and Ni1−P 2.208 Å) are elongated compared to **1**, most likely caused by the higher coordination number of the Ni atom. In comparison with the cationic complexes [**1**]BF_4 and [**1**(THF)]PF_6, [**1**]Br displays similar Ni−P distances but shortened Ni−N distances. The Ni1−Br1 bond length of 2.4889(4) Å is in the range of covalent Ni−Br bonds (sum of covalent radii 2.430 Å),[77] while the geometry index of τ_5 = 0.79 is consistent with a distorted trigonal-bipyramidal structure (Table 1). The magnetic moment of [**1**]Br [2.1(1) μ_B in THF-d_8 at 300 K] was determined by the Evans NMR method and is consistent with an $S = {}^1/_2$ Ni(I) center (Table 1). Additionally, EPR measurements in a toluene glass at 20 K indicate the presence of a Ni(I) species with a metal-centered radical (Figure S24; simulated **g** tensor: g_{11} = 2.190, g_{22} = 2.125, and g_{33} = 2.060), similar to [**1**]BF_4 and [**1**(THF)]PF_6. The calculated spin density on Ni (0.82) as well as the calculated **g** tensor are in good agreement with the experimental data (Table S5).

Although Ni-mediated cross-coupling reactions usually involve Ni(0) and Ni(II) species,[79] Ni(I) complexes analogous to [**1**]Br have also been suggested as viable intermediates and may also show pronounced catalytic activity.[80−84] Some other nickel(I) halide complexes have also been isolated from the reaction of Ni(0) complexes with PhX.[85,86]

The reaction of **1** was also investigated toward 1 equiv of iodobenzene under analogous conditions (toluene, 60 °C) but was found to lead to a significantly different outcome. In this case, full consumption (>99%) of iodobenzene took place according to GC-FID analysis. Compound **2** could again be isolated after extraction with *n*-hexane. However, the remaining residue showed a deep-green color rather than deep red, as had been observed using PhBr. Crystals were obtained from a toluene solution of this residue, after layering with *n*-hexane. Single-crystal XRD revealed a new product **3**, which shows a significantly different structure in the solid state than [**1**]Br (Figure 5). Most notably, **3** has clearly lost one of its phosphinine ligands **L**. Moreover, the Ni center—which is tetrahedrally coordinated (τ_4 = 0.95; Table 1)—is bound to *two* iodide ligands, as well as by a formally anionic 1-Ph-λ^4-phosphinine ligand, which is derived by the addition of an extra phenyl substituent to ligand **L**. The Ni1−P1 distance [2.2509(6) Å] is in the range of Ni−P single bonds (sum of covalent radii 2.21 Å), while the Ni1−N1 [1.9941(19) Å] bond length is elongated in a manner similar to in **1**. The Ni1−I distances (mean value 2.514 Å) are in the range of typical Ni−I bonds (sum of covalent radii 2.43 Å). We anticipate that **3** is formed by oxidative addition of the carbon−halogen bond to the Ni center and subsequent transfer of the aryl fragment to the ligand. A similar reaction of a (TPP)Ni(C_2H_5)(acac) complex (TPP = 2,4,6-triphenylphosphinine; acac = acetylacetonate) has been proposed by Lehmkuhl et al.[23]

Unlike [**1**]Br, the electronic structure of **3** cannot be assigned easily. The measured value of the magnetic moment

https://dx.doi.org/10.1021/acs.inorgchem.0c01115
Inorg. Chem. 2020, 59, 9951−9961

[3.2(1) in THF-d_8 at 300 K] lies between those expected for two and three unpaired electrons (Table 1). The magnetic susceptibility of a solid sample of **3** was measured with a SQUID magnetometer in the temperature range 100 K < T < 400 K. The results are shown in Figure 6. These data reveal

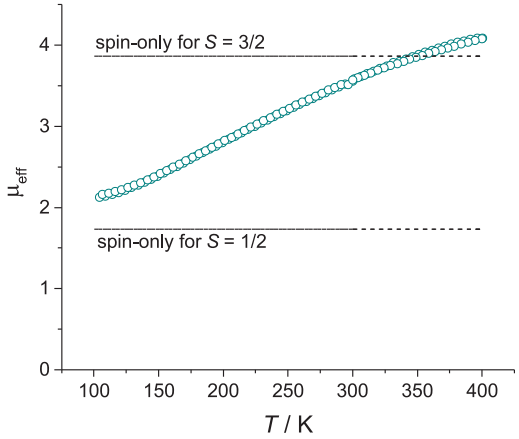

Figure 6. Magnetic susceptibility data recorded for a solid sample of **3** in the temperature range 100−400 K in the heating and cooling mode and an applied field of 5000 Oe.

that the magnetic moment continuously increases from μ_{eff} = 2 at 105 K to 4 at 400 K. These data suggest that a thermally activated spin transition occurs from an $S = {}^1/_2$ ground state into an $S = {}^3/_2$ excited state. The latter dominates at the upper limit of the accessible temperature window. In addition, it is noteworthy that the measured effective moment significantly exceeds the expected spin-only value for an $S = {}^3/_2$ system at high temperature (T > 350 K). This observation might be explained by unquenched orbital contributions to the magnetic moment of the $S = {}^3/_2$ species, which is a common phenomenon for complexes with a tetrahedral d^8 configuration at the metal atom.[87]

The EPR spectrum of **3** recorded at 20 K in a toluene glass shows overlapping and broad signals for the **g** tensors. The simulated **g** tensor (g_{11} = 2.390, g_{22} = 2.242, and g_{33} = 2.120) is consistent with a Ni-centered radical in a rhombic $S = {}^1/_2$ system (Figure 7).

In the case of **3**, the experimental data could not be reproduced in good agreement using standard DFT (for details, see the SI). Furthermore, a rather large spin density was calculated at the Ni atom (1.23), hinting at a broken-symmetry solution. Indeed, a broken-symmetry treatment at the TPSS0-D3BJ/def2-TZVP level shows an interesting electronic structure. Here, an intermediate-spin Ni center (S = 1, d^8) is antiferromagnetically coupled to a phosphacyclohexadienyl radical, resulting in an overall $S = {}^1/_2$ species (**3-II**; for details, see the SI). A small energy separation between the broken-symmetry doublet and quartet states was calculated by DFT ($\Delta E_{doublet-quartet}$ = 1.1 kcal·mol^{-1} at the TPSS0-D3BJ/def2-TZVP level of theory). However, dedicated multireference calculations, namely, CASSCF-NEVPT2 with an active space of 13 electrons in 12 orbitals, reveal a much more complicated electronic structure of the $S = {}^1/_2$ ground state of **3**. These calculations show that all three mesomeric structures (**3-I**, **3-II**, and **3-III**), shown in Scheme 3 (vide supra), contribute significantly to the overall electronic structure of **3**. Thus, **3** exhibits significant multireference character, which

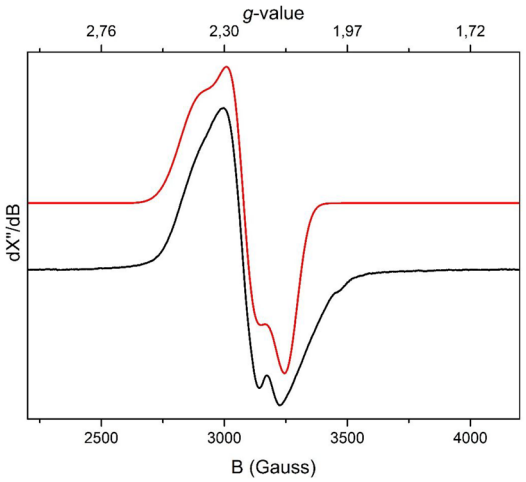

Figure 7. Experimental (black) and simulated (red) EPR spectra of **3** recorded at 20 K in a toluene glass. Simulation parameters: g_{11} = 2.390, g_{22} = 2.242, and g_{33} = 2.120; W_{11} = 90, W_{22} = 55, and W_{33} = 55. Experimental conditions: microwave frequencies 9.644902 GHz; power 0.6325 mW; modulation amplitude 2.000 G.

makes an assignment of the oxidation state of the Ni atom somewhat ambiguous. However, both broken-symmetry DFT and CASSCF clearly show the redox-active behavior of the anionic 1-phenylphosphacyclohexadienyl ligand in **3**. Furthermore, the CASSCF-NEVPT2 estimation of the **g** tensor is in qualitative agreement with the experiment and reproduces the observed significant anisotropy of the **g** tensor (g_z = 2.562, g_y = 2.227, and g_x = 2.173).

CONCLUSION

In summary, we have presented the synthesis and crystallographic characterization of the homoleptic 2-(2′-pyridyl)-4,6-phosphininenickel(0) complex **1**. First reactivity studies on the phosphinine-based Ni complex **1** show that it can be conveniently oxidized using ferrocenium salts FcX. Oxidation with $FcBF_4$ and $FcPF_6$ leads to the formation of Ni(I) complexes [**1**]BF_4 and [**1**(THF)]PF_6, which possess similar trigonal-bipyramidal structural motifs. Oxidation of **1** with $FcBAr^F{}_4$, on the other hand, affords a dicationic dinuclear Ni(I) complex [$\mathbf{1}_2$]($BAr^F{}_4$)$_2$ containing a bridging phosphinine ligand in the rare μ_2-coordination mode. The reaction of **1** with bromobenzene leads to formation of the λ^5-phosphinine **2** and the trigonal-bipyramidal Ni(I) complex [**1**]Br. In contrast, the reaction of **1** with iodobenzene results in the formation of **2** and the tetrahedral Ni complex **3**, which is based on a formally anionic 1-Ph-λ^4-phosphinine. Quantum-chemical calculations on **3** highlight the redox-active behavior of the phosphinine moiety, which prohibits a clear assignment of an oxidation state to the Ni center. The carbon−halogen bond splitting by a transition-metal complex and transfer of the aryl fragment to the ligand highlight the chemical noninnocence of phosphinine ligands in transition-metal complexes. Investigations on the mechanism of formation of [**1**]Br and **3** and further reactivity studies on **1** are currently underway in our laboratories.

ASSOCIATED CONTENT

Supporting Information

The Supporting Information is available free of charge at https://pubs.acs.org/doi/10.1021/acs.inorgchem.0c01115.

https://dx.doi.org/10.1021/acs.inorgchem.0c01115
Inorg. Chem. 2020, 59, 9951−9961

Full synthetic details, NMR, UV−vis, and EPR spectra, and crystallographic refinement and computational details (PDF)

Accession Codes

CCDC 2007973 and 1988434−1988439 contain the supplementary crystallographic data for this paper. These data can be obtained free of charge via www.ccdc.cam.ac.uk/data_request/cif, or by emailing data_request@ccdc.cam.ac.uk, or by contacting The Cambridge Crystallographic Data Centre, 12 Union Road, Cambridge CB2 1EZ, UK; fax: +44 1223 336033.

AUTHOR INFORMATION

Corresponding Authors

R. Wolf − *Institute of Inorganic Chemistry, Universität Regensburg, 93040 Regensburg, Germany*; Email: robert.wolf@ur.de

B. de Bruin − *van't Hoff Institute for Molecular Sciences, University of Amsterdam, 1098 XH Amsterdam, The Netherlands*; orcid.org/0000-0002-3482-7669; Email: b.debruin@uva.nl

C. Müller − *Institute of Chemistry and Biochemistry, Freie Universität Berlin, 14195 Berlin, Germany*; Email: c.mueller@fu-berlin.de

Authors

J. Leitl − *Institute of Inorganic Chemistry, Universität Regensburg, 93040 Regensburg, Germany*

P. Coburger − *Institute of Inorganic Chemistry, Universität Regensburg, 93040 Regensburg, Germany*

D. J. Scott − *Institute of Inorganic Chemistry, Universität Regensburg, 93040 Regensburg, Germany*

C. G. P. Ziegler − *Institute of Inorganic Chemistry, Universität Regensburg, 93040 Regensburg, Germany*

G. Hierlmeier − *Institute of Inorganic Chemistry, Universität Regensburg, 93040 Regensburg, Germany*

N. P. van Leest − *van't Hoff Institute for Molecular Sciences, University of Amsterdam, 1098 XH Amsterdam, The Netherlands*

G. Hörner − *Department of Chemistry, Inorganic Chemistry IV, Unversität Bayreuth, 95440 Bayreuth, Germany*; orcid.org/0000-0002-3883-2879

Complete contact information is available at: https://pubs.acs.org/10.1021/acs.inorgchem.0c01115

Notes

The authors declare no competing financial interest.

ACKNOWLEDGMENTS

We thank Prof. Birgit Weber (Universität Bayreuth, Bayreuth, Germany) for access to a SQUID magnetometer and helpful discussions. Funding by the Deutsche Forschungsgemeinschaft (Grants WO1496/9-1 and MU1657/5-1) and Alexander von Humboldt Foundation (postdoctoral fellowship to D.J.S.) is gratefully acknowledged.

REFERENCES

(1) Tasker, S. Z.; Standley, E. A.; Jamison, T. F. Recent Advances in Homogeneous Nickel Catalysis. *Nature* **2014**, *509* (7500), 299−309.

(2) Wender, P. A.; Smith, T. E.; Zuo, G.; Duong, H. A.; Louie, J. Bis(1,5-Cyclooctadiene)Nickel(0). *Encyclopedia of Reagents for Organic Synthesis*; American Cancer Society, 2006.

(3) Binger, P.; McMeeking, J. Codimerization of 3,3-Dimethylcyclopropene with Ethylenecarboxylic Esters at Nickel(0) Catalysts. *Angew. Chem., Int. Ed. Engl.* **1974**, *13* (7), 466−467.

(4) Binger, P.; Brinkmann, A. Cyclische Ketone aus 3,3-Dimethyl-1-cyclopropen und Kohlenmonoxid durch katalysierte Cotrimerisation. *Chem. Ber.* **1978**, *111* (7), 2689−2695.

(5) Heimbach, P.; Ploner, K.-J.; Thömel, F. Preparation of Substituted 5-Vinylcyclohexa-1,3-Dienes and Tricyclo[2.2.2.02,6]-Oct-7-Enes. *Angew. Chem., Int. Ed. Engl.* **1971**, *10* (4), 276−277.

(6) Binger, P.; Schroth, G.; McMeeking, J. Quantitative Cyclotrimerization of 3,3-Dimethylcyclo-Propene to "Hexamethy1-Trans-σ-Trishomobenzene. *Angew. Chem., Int. Ed. Engl.* **1974**, *13* (7), 465−466.

(7) Fahey, D. R. Synthesis of 5-Vinylcyclohexa-1,3-Diene by a Nickel-Catalyzed Cooligomerization of Acetylene and Butadiene. *J. Org. Chem.* **1972**, *37* (26), 4471−4473.

(8) Tamao, K.; Kiso, Y.; Sumitani, K.; Kumada, M. Alkyl Group Isomerization in the Cross-Coupling Reaction of Secondary Alkyl Grignard Reagents with Organic Halides in the Presence of Nickel-Phosphine Complexes as Catalysts. *J. Am. Chem. Soc.* **1972**, *94* (26), 9268−9269.

(9) Budnikova, Yu. G.; Kargin, Yu. M.; Yanilkin, V. V. Dimer Formation in the Reaction of Aryl Halides Catalyzed by Nickel Complexes. *Russ. Chem. Bull.* **1992**, *41* (7), 1299−1300.

(10) Budnikova, Yu. G.; Kargin, Yu. M. Electrochemical Reduction of Halopyridines Catalyzed by $Ni^0(Bipy)_2$. *Russ. J. Gen. Chem.* **2001**, *71* (1), 128−131.

(11) Rollin, Y.; Troupel, M.; Tuck, D. G.; Perichon, J. The Coupling of Organic Groups by the Electrochemical Reduction of Organic Halides: Catalysis by 2,2′-Bipyridinenickel Complexes. *J. Organomet. Chem.* **1986**, *303* (1), 131−137.

(12) Yakhvarov, D. G.; Hey-Hawkins, E.; Kagirov, R. M.; Budnikova, Yu. H.; Ganushevich, Yu. S.; Sinyashin, O. G. Electrocatalytic Reduction of Aryldichlorophosphines with the (2,2′-Bipyridine) Nickel Complexes. *Russ. Chem. Bull.* **2007**, *56* (5), 935−942.

(13) Gelman, D.; Dechert, S.; Schumann, H.; Blum, J. 2,2′-Bipyridine, 2-(2-Oxazolyl)Pyridine and 2,2′-Bisoxazole Derived Nickel(0) Complexes as Selective Catalysts for Cross-Coupling of Aryl Chlorides by Intramolecularly Stabilized Dialkylaluminum Reagents. *Inorg. Chim. Acta* **2002**, *334*, 149−158.

(14) Le Floch, P.; Carmichael, D.; Ricard, L.; Mathey, F. Synthesis of the First 2,2'-Biphosphinine. X-Ray Crystal Structure Analysis of Its Tetracarbonylchromium Complex. *J. Am. Chem. Soc.* **1991**, *113* (2), 667−669.

(15) Le Floch, P.; Carmichael, D.; Ricard, L.; Mathey, F.; Jutand, A.; Amatore, C. Structural and Electrochemical Study of a 2,2'-Biphosphinine. *Organometallics* **1992**, *11* (7), 2475−2479.

(16) Rosa, P.; Ricard, L.; Mathey, F.; Le Floch, P. A 2,2′-Biphosphinine Dianion: Synthesis and Reactivity. *Organometallics* **1999**, *18* (17), 3348−3352.

(17) Mézailles, N.; Rosa, P.; Ricard, L.; Mathey, F.; Le Floch, P. Biphosphinine Rhodium and Cobalt(−1) Complexes. *Organometallics* **2000**, *19* (16), 2941−2943.

(18) Choua, S.; Sidorenkova, H.; Berclaz, T.; Geoffroy, M.; Rosa, P.; Mézailles, N.; Ricard, L.; Mathey, F.; Le Floch, P. One-Electron Reduction Product of a Biphosphinine Derivative and of Its Ni(0) Complex: Crystal Structure, EPR/ENDOR, and DFT Investigations on $(Tmbp)^{\bullet-}$ and $[Ni(Tmbp)_2]^{\bullet-}$. *J. Am. Chem. Soc.* **2000**, *122* (49), 12227−12234.

(19) Elschenbroich, C.; Nowotny, M.; Behrendt, A.; Massa, W.; Wocadlo, S. Tetrakis(H1-Phosphabenzene)Nickel. *Angew. Chem., Int. Ed. Engl.* **1992**, *31* (10), 1343−1345.

(20) Lehmkuhl, H.; Paul, R.; Mynott, R. Phosphabenzolnickel-Komplexe. *Liebigs Ann. Chem.* **1981**, *1981* (6), 1139−1146.

(21) Mézailles, N.; Le Floch, P.; Waschbüsch, K.; Ricard, L.; Mathey, F.; Kubiak, C. P. Synthesis and X-Ray Crystal Structures of Dimeric Nickel(0) and Tetrameric Copper(I) Iodide Complexes of 2-Diphenylphosphino-3-Methylphosphinine. *J. Organomet. Chem.* **1997**, *541* (1), 277−283.

(22) Holah, D. G.; Hughes, A. N.; Knudsen, K. L.; Perrier, R. The Synthesis and Some NMR Properties of 2,3-Bis(Diphenylphosphino)-6-Phenyl-Λ3-Phosphinine. *J. Heterocycl. Chem.* **1988**, *25* (1), 155−160.
(23) Lehmkuhl, H.; Paul, R.; Krüger, C.; Tsay, Y.-H.; Benn, R.; Mynott, R. 1,2,4,6-Tetraorganophosphorinylnickel-Komplexe. *Liebigs Ann. Chem.* **1981**, *1981* (6), 1147−1161.
(24) Lehmkuhl, H.; Elsäßer, J.; Benn, R.; Gabor, B.; Rufińska, A.; Goddard, R.; Krüger, C. Ein-Und Zweikernige Phosphorinylnickel-Komplexe/Mono-and Binuclear Phosphorinylnickel Complexes. *Z. Naturforsch., B: J. Chem. Sci.* **1985**, *40* (2), 171−181.
(25) Mathey, F.; Le Floch, P. Phosphorus Analogs of Bipyridines: Their Synthesis and Coordination Chemistry. *Chem. Ber.* **1996**, *129* (3), 263−268.
(26) Le Floch, P.; Carmichael, D.; Ricard, L.; Mathey, F. Synthesis of the First 2,2'-Biphosphinine. X-Ray Crystal Structure Analysis of Its Tetracarbonylchromium Complex. *J. Am. Chem. Soc.* **1991**, *113* (2), 667−669.
(27) LeFloch, P.; Ricard, L.; Mathey, F.; Jutand, A.; Amatore, C. Use of 2,2'-Biphosphinines for the Stabilization of Reduced Transition Metal Species: Electrochemical Reduction of Bis(2,2'-biphosphinine)-nickel(0). *Inorg. Chem.* **1995**, *34* (1), 11−12.
(28) Rosa, P.; Mézailles, N.; Mathey, F.; Le Floch, P. Nickel(II)-Promoted Homocoupling Reaction of 2-(Phosphininyl)-Halogenozirconocene Complexes: A New and Efficient Synthesis of 2,2′-Biphosphinines. *J. Org. Chem.* **1998**, *63* (14), 4826−4828.
(29) See ref 28 for oxidative reactions of Ni(biphosphinine)$_2$ complexes with C_2Cl_6.
(30) Müller, C.; Wasserberg, D.; Weemers, J. J. M.; Pidko, E. A.; Hoffmann, S.; Lutz, M.; Spek, A. L.; Meskers, S. C. J.; Janssen, R. A. J.; van Santen, R. A.; Vogt, D. Donor-Functionalized Polydentate Pyrylium Salts and Phosphinines: Synthesis, Structural Characterization, and Photophysical Properties. *Chem. - Eur. J.* **2007**, *13* (16), 4548−4559.
(31) Müller, C.; Vogt, D. Recent Developments in the Chemistry of Donor-Functionalized Phosphinines. *C. R. Chim.* **2010**, *13* (8), 1127−1143.
(32) Müller, C.; Sklorz, J. A. W.; de Krom, I.; Loibl, A.; Habicht, M.; Bruce, M.; Pfeifer, G.; Wiecko, J. Recent Developments in the Chemistry of Pyridyl-Functionalized, Low-Coordinate Phosphorus Heterocycles. *Chem. Lett.* **2014**, *43* (9), 1390−1404.
(33) Carrasco, A. C.; Pidko, E. A.; Masdeu-Bultó, A. M.; Lutz, M.; Spek, A. L.; Vogt, D.; Müller, C. 2-(2′-Pyridyl)-4,6-Diphenylphosphinine versus 2-(2′-Pyridyl)-4,6-Diphenylpyridine: An Evaluation of Their Coordination Chemistry towards Rh(I). *New J. Chem.* **2010**, *34* (8), 1547−1550.
(34) Campos-Carrasco, A.; Broeckx, L. E. E.; Weemers, J. J. M.; Pidko, E. A.; Lutz, M.; Masdeu-Bultó, A. M.; Vogt, D.; Müller, C. Pd^{II} and Pt^{II} Complexes of 2-(2′-Pyridyl)-4,6-Diphenylphosphinine: Synthesis, Structure, and Reactivity. *Chem. - Eur. J.* **2011**, *17* (8), 2510−2517.
(35) de Krom, I.; Pidko, E. A.; Lutz, M.; Müller, C. Reactions of Pyridyl-Functionalized, Chelating λ^3-Phosphinines in the Coordination Environment of Rh^{III} and Ir^{III}. *Chem. - Eur. J.* **2013**, *19* (23), 7523−7531.
(36) Pfeifer, G.; Ribagnac, P.; Le Goff, X.-F.; Wiecko, J.; Mézailles, N.; Müller, C. Reactivity of Aromatic Phosphorus Heterocycles - Differences Between Nonfunctionalized and Pyridyl-Substituted 2,4,6-Triarylphosphinines. *Eur. J. Inorg. Chem.* **2015**, *2015* (2), 240−249.
(37) Loibl, A.; Weber, M.; Lutz, M.; Müller, C. Re^{I} Complexes of Pyridylphosphinines and 2,2′-Bipyridine Derivatives: A Comparison. *Eur. J. Inorg. Chem.* **2019**, *2019*, 1575−1585.
(38) de Krom, I.; Broeckx, L. E. E.; Lutz, M.; Muller, C. 2-(2′-Pyridyl)-4,6-Diphenylphosphinine versus 2-(2′-Pyridyl)-4,6-Diphenylpyridine: Synthesis, Characterization, and Reactivity of Cationic Rh^{III} and Ir^{III} Complexes Based on Aromatic Phosphorus Heterocycles. *Chem. - Eur. J.* **2013**, *19* (11), 3676−3684.
(39) Loibl, A.; de Krom, I.; Pidko, E. A.; Weber, M.; Wiecko, J.; Müller, C. Tuning the Electronic Effects of Aromatic Phosphorus Heterocycles: An Unprecedented Phosphinine with Significant P(π)-Donor Properties. *Chem. Commun.* **2014**, *50* (64), 8842−8844.
(40) Loibl, A.; Oschmann, W.; Vogler, M.; Pidko, E. A.; Weber, M.; Wiecko, J.; Müller, C. Substituent Effects in Pyridyl-Functionalized Pyrylium Salts, Pyridines and λ^3,σ^2-Phosphinines: A Fundamental and Systematic Study. *Dalton Trans.* **2018**, *47* (28), 9355−9366.
(41) de Krom, I.; Lutz, M.; Müller, C. 2-(2′-Pyridyl)-4,6-Diphenylphosphinine versus 2-(2′-Pyridyl)-4,6-Diphenylpyridine: Synthesis and Characterization of Novel Cr^0, Mo^0 and W^0 Carbonyl Complexes Containing Chelating P, N and N, N Ligands. *Dalton Trans.* **2015**, *44* (22), 10304−10314.
(42) Leitl, J.; Marquardt, M.; Coburger, P.; Scott, D. J.; Streitferdt, V.; Gschwind, R. M.; Müller, C.; Wolf, R. Facile C = O Bond Splitting of Carbon Dioxide Induced by Metal-Ligand Cooperativity in a Phosphinine Iron(0) Complex. *Angew. Chem., Int. Ed.* **2019**, *58* (43), 15407−15411.
(43) Elsby, M. R.; Johnson, S. A. Nickel-Catalyzed C-H Silylation of Arenes with Vinylsilanes: Rapid and Reversible β-Si Elimination. *J. Am. Chem. Soc.* **2017**, *139* (27), 9401−9407.
(44) Hua, C.; DeGayner, J. A.; Harris, T. D. Thiosemiquinoid Radical-Bridged Cr^{III}_2 Complexes with Strong Magnetic Exchange Coupling. *Inorg. Chem.* **2019**, *58* (10), 7044−7053.
(45) Deb, M.; Hazra, S.; Dolui, P. A.; Elias, J. Ferrocenium Promoted Oxidation of Benzyl Amines to Imines Using Water as the Solvent and Air as the Oxidant. *ACS Sustainable Chem. Eng.* **2019**, *7* (1), 479−486.
(46) (a) *SCALE3ABS, CrysAlisPro*; Aglient Technologies Inc.: Oxford, U.K., 2012. (b) Sheldrick, G. M. *SADABS*; Bruker AXS: Madison, WI, 2007.
(47) Clark, R. C.; Reid, J. S. The analytical calculation of absorption in multifaceted crystals. *Acta Crystallogr., Sect. A: Found. Crystallogr.* **1995**, *51*, 887−897.
(48) Sheldrick, G. M. Crystal structure refinement with SHELXL. *Acta Crystallogr., Sect. C: Struct. Chem.* **2015**, *71*, 3−8.
(49) Sheldrick, G. M. A short history of SHELX. *Acta Crystallogr., Sect. A: Found. Crystallogr.* **2008**, *64*, 112−122.
(50) Carmichael, D.; Le Floch, P.; Ricard, L.; Mathey, F. Ruthenium(II) Complexes of a 2,2′-Biphosphinine. *Inorg. Chim. Acta* **1992**, *198−200*, 437−441.
(51) Breque, A.; Santini, C. C.; Mathey, F.; Fischer, J.; Mitschler, A. 4,5-Dimethyl-2-(2-Pyridyl)Phosphorin as a Chelating Ligand. Synthesis and x-Ray Crystal Structure Analysis of (4,5-Dimethyl-2-(2-Pyridyl)Phosphorin)Tetracarbonylchromium. *Inorg. Chem.* **1984**, *23* (22), 3463−3467.
(52) Le Floch, P.; Mansuy, S.; Ricard, L.; Mathey, F.; Jutand, A.; Amatore, C. Synthesis, Structure, Reactivity, and Electrochemical Study of a (2,2′-Biphosphinine)(H5-Pentamethylcyclo- Pentadienyl)-Chlororuthenium(II) Complex. *Organometallics* **1996**, *15* (15), 3267−3274.
(53) Kaes, C.; Katz, A.; Hosseini, M. W. Bipyridine: The Most Widely Used Ligand. A Review of Molecules Comprising at Least Two 2,2′-Bipyridine Units. *Chem. Rev.* **2000**, *100* (10), 3553−3590.
(54) M, D.; M, D.; J, P. Investigation of the Reductive Coupling of Aryl Halides and/or Ethylchloroacetate Electrocatalyzed by the Precursor NiX_2(Bpy) with X^-=Cl^-, Br^- or $MeSO_3^-$ and Bpy = 2,2′-Dipyridyl. *New J. Chem.* **1996**, *20* (6), 659−667.
(55) Okuniewski, A.; Rosiak, D.; Chojnacki, J.; Becker, B. Coordination Polymers and Molecular Structures among Complexes of Mercury(II) Halides with Selected 1-Benzoylthioureas. *Polyhedron* **2015**, *90*, 47−57.
(56) Addison, A. W.; Rao, T. N.; Reedijk, J.; van Rijn, J.; Verschoor, G. C. Synthesis, Structure, and Spectroscopic Properties of Copper(II) Compounds Containing Nitrogen-Sulphur Donor Ligands; the Crystal and Molecular Structure of Aqua[1,7-Bis(N-Methylbenzimidazol-2′-Yl)-2,6-Dithiaheptane]Copper(II) Perchlorate. *J. Chem. Soc., Dalton Trans.* **1984**, 1349−1356.
(57) Schmid, B.; Venanzi, L. M.; Gerfin, T.; Gramlich, V.; Mathey, F. Synthesis and Spectroscopic Properties of the Complexes $[M_2(DIEN)_2(NIPHOS)_2][SbF_6]_2$ (M = Ir, DIEN = 1,5-Cyclo-

https://dx.doi.org/10.1021/acs.inorgchem.0c01115
Inorg. Chem. 2020, 59, 9951−9961

octadiene (COD); M = Rh, DIEN = Norbornadiene (NBD); NIPHOS = 2-(2′-Pyridyl)-4,5-Dimethylphosphinine). X-Ray Crystal Structure of $[Ir_2(COD)_2(NIPHOS)_2][SbF_6]_2$. *Inorg. Chem.* **1992**, *31* (24), 5117−5122.
(58) Reetz, M. T.; Bohres, E.; Goddard, R.; Holthausen, M. C.; Thiel, W. Synthesis, Solid-State Structure, and Electronic Nature of a Phosphinine-Stabilized Triangulo Palladium Cluster. *Chem. - Eur. J.* **1999**, *5* (7), 2101−2108.
(59) Bakker, M. J.; Vergeer, F. W.; Hartl, F.; Rosa, P.; Ricard, L.; Le Floch, P.; Calhorda, M. J. Bonding and Redox Properties of $[Os_3(CO)_9(Tmbp)(L)]$ (Tmbp = 4,4′,5,5′-Tetramethyl-2,2′-Biphosphinine; L = CO, PPh_3) Clusters with an Unprecedented Electron-Deficient Metallic Core and Doubly Bridging Biphosphinine Dianion. *Chem. - Eur. J.* **2002**, *8* (7), 1741−1752.
(60) Elschenbroich, C.; Six, J.; Harms, K. On a Novel Coordination Mode of Phosphinine C_5H_5P. *Chem. Commun.* **2006**, No. 32, 3429−3431.
(61) Chen, X.; Li, Z.; Yanan, F.; Grützmacher, H. Synthesis and Photoluminescence Properties of Cu^I Complexes with Chelating Phosphinito Phosphinine Ligands. *Eur. J. Inorg. Chem.* **2016**, *2016* (5), 633−638.
(62) Rosa, P.; Ricard, L.; Mathey, F.; Le Floch, P. Syntheses and X-Ray Structures of (2,2′-Biphosphinine)-(H_5-Pentamethylcyclopentadienyl)Ruthenium(I) Dimer and Ruthenium(0) Complexes. *Organometallics* **2000**, *19* (24), 5247−5250.
(63) Habicht, M. H.; Wossidlo, F.; Bens, T.; Pidko, E. A.; Müller, C. 2-(Trimethylsilyl)-λ^3-Phosphinine: Synthesis, Coordination Chemistry, and Reactivity. *Chem. - Eur. J.* **2018**, *24* (4), 944−952.
(64) Hou, Y.; Li, Z.; Li, Y.; Liu, P.; Su, C.-Y.; Puschmann, F.; Grützmacher, H. Making the Unconventional μ_2-P Bridging Binding Mode More Conventional in Phosphinine Complexes. *Chem. Sci.* **2019**, *10* (11), 3168−3180.
(65) Mao, Y.; Lim, K. M. H.; Li, Y.; Ganguly, R.; Mathey, F. The Original Coordination Chemistry of 2-Phosphaphenol with Copper(I) and Gold(I) Halides. *Organometallics* **2013**, *32* (12), 3562−3565.
(66) Zhao, X.; Sun, X.; Han, Z.; Zhao, C.; Yu, H.; Zhai, X. Two New Polyoxometalate-Based Hybrids Consisting of Keggin-Type Cluster Modified by $\{Ag_4\}$ Group. *J. Solid State Chem.* **2013**, *207*, 178−183.
(67) Fedushkin, I. L.; Petrovskaya, T. V.; Girgsdies, F.; Köhn, R. D.; Bochkarev, M. N.; Schumann, H. Synthesis and Structure of the First Lanthanide Complex with the Bridging, Antiaromatic 2,2′-Bipyridine Dianion: $[Yb(M_2\text{-}N_2C_{10}H_8)(Thf)_{23}]$. *Angew. Chem., Int. Ed.* **1999**, *38* (15), 2262−2264.
(68) Gore-Randall, E.; Irwin, M.; Denning, M. S.; Goicoechea, J. M. Synthesis and Characterization of Alkali-Metal Salts of 2,2′- and 2,4′-Bipyridyl Radicals and Dianions. *Inorg. Chem.* **2009**, *48* (17), 8304−8316.
(69) Tasker, S. Z.; Standley, E. A.; Jamison, T. F. Recent Advances in Nickel Catalysis. *Nature* **2014**, *509* (7500), 299−309.
(70) Ananikov, V. P. Nickel: The "Spirited Horse" of Transition Metal Catalysis. *ACS Catal.* **2015**, *5* (3), 1964−1971.
(71) Tamao, K.; Sumitani, K.; Kumada, M. Selective Carbon-Carbon Bond Formation by Cross-Coupling of Grignard Reagents with Organic Halides. Catalysis by Nickel-Phosphine Complexes. *J. Am. Chem. Soc.* **1972**, *94* (12), 4374−4376.
(72) Guo, L.; Srimontree, W.; Zhu, C.; Maity, B.; Liu, X.; Cavallo, L.; Rueping, M. Nickel-Catalyzed Suzuki-Miyaura Cross-Couplings of Aldehydes. *Nat. Commun.* **2019**, *10* (1), 1−6.
(73) Hashimoto, N.; Umano, R.; Ochi, Y.; Shimahara, K.; Nakamura, J.; Mori, S.; Ohta, H.; Watanabe, Y.; Hayashi, M. Synthesis and Photophysical Properties of Λ5-Phosphinines as a Tunable Fluorophore. *J. Am. Chem. Soc.* **2018**, *140* (6), 2046−2049.
(74) Huang, J.; Tarábek, J.; Kulkarni, R.; Wang, C.; Dračínský, M.; Smales, G. J.; Tian, Y.; Ren, S.; Pauw, B. R.; Resch-Genger, U.; Bojdys, M. J. A π-Conjugated, Covalent Phosphinine Framework. *Chem. - Eur. J.* **2019**, *25* (53), 12342−12348.
(75) Yoshimura, A.; Kimura, H.; Handa, A.; Hashimoto, N.; Yano, M.; Mori, S.; Shirahata, T.; Hayashi, M.; Misaki, Y. Synthesis, Structures, and Electrochemical and Optical Properties of λ^5-Phosphinine Derivatives Functionalized Tetrathiafulvalene Analogs. *Tetrahedron Lett.* **2020**, *61*, 151724.
(76) Pfeifer, G.; Chahdoura, F.; Papke, M.; Weber, M.; Szücs, R.; Geffroy, B.; Tondelier, D.; Nyulászi, L.; Hissler, M.; Müller, C. Synthesis, Electronic Properties and OLED Devices of Chromophores Based on λ^5-Phosphinines. *Chem. - Eur. J.* **2020**, DOI: 10.1002/chem.202000932.
(77) Pyykko, P.; Atsumi, M. Molecular Double-Bond Covalent Radii for Elements Li-E112. *Chem. - Eur. J.* **2009**, *15* (46), 12770−12779.
(78) Sklorz, J. A. W.; Hoof, S.; Rades, N.; De Rycke, N.; Könczöl, L.; Szieberth, D.; Weber, M.; Wiecko, J.; Nyulászi, L.; Hissler, M.; Müller, C. Pyridyl-Functionalised 3H-1,2,3,4-Triazaphospholes: Synthesis, Coordination Chemistry and Photophysical Properties of Low-Coordinate Phosphorus Compounds. *Chem. - Eur. J.* **2015**, *21* (31), 11096−11109.
(79) Foà, M.; Cassar, L. Oxidative Addition of Aryl Halides to Tris(Triphenylphosphine)Nickel(0). *J. Chem. Soc., Dalton Trans.* **1975**, *23*, 2572−2576.
(80) Schley, N. D.; Fu, G. C. Nickel-Catalyzed Negishi Arylations of Propargylic Bromides: A Mechanistic Investigation. *J. Am. Chem. Soc.* **2014**, *136* (47), 16588−16593.
(81) Cornella, J.; Gómez-Bengoa, E.; Martin, R. Combined Experimental and Theoretical Study on the Reductive Cleavage of Inert C-O Bonds with Silanes: Ruling out a Classical Ni(0)/Ni(II) Catalytic Couple and Evidence for Ni(I) Intermediates. *J. Am. Chem. Soc.* **2013**, *135* (5), 1997−2009.
(82) Guard, L. M.; Mohadjer Beromi, M.; Brudvig, G. W.; Hazari, N.; Vinyard, D. J. Comparison of Dppf-Supported Nickel Precatalysts for the Suzuki-Miyaura Reaction: The Observation and Activity of Nickel(I). *Angew. Chem., Int. Ed.* **2015**, *54* (45), 13352−13356.
(83) Mohadjer Beromi, M.; Nova, A.; Balcells, D.; Brasacchio, A. M.; Brudvig, G. W.; Guard, L. M.; Hazari, N.; Vinyard, D. J. Mechanistic Study of an Improved Ni Precatalyst for Suzuki-Miyaura Reactions of Aryl Sulfamates: Understanding the Role of Ni(I) Species. *J. Am. Chem. Soc.* **2017**, *139* (2), 922−936.
(84) Kalvet, I.; Guo, Q.; Tizzard, G. J.; Schoenebeck, F. When Weaker Can Be Tougher: The Role of Oxidation State (I) in P- *vs* N-Ligand-Derived Ni-Catalyzed Trifluoromethylthiolation of Aryl Halides. *ACS Catal.* **2017**, *7* (3), 2126−2132.
(85) Funes-Ardoiz, I.; Nelson, D. J.; Maseras, F. Halide Abstraction Competes with Oxidative Addition in the Reactions of Aryl Halides with $[Ni(PMenPh(3\text{-}n))_4]$. *Chem. - Eur. J.* **2017**, *23* (66), 16728−16733.
(86) Nelson, D. J.; Maseras, F. Steric Effects Determine the Mechanisms of Reactions between Bis(N-Heterocyclic Carbene)-Nickel(0) Complexes and Aryl Halides. *Chem. Commun.* **2018**, *54* (75), 10646−10649.
(87) Kahn, O.; *Molecular Magnetism*; VCH Publishers: New York, 1993.

https://dx.doi.org/10.1021/acs.inorgchem.0c01115
Inorg. Chem. 2020, 59, 9951−9961